Crystallization and Melting Behavior of Poly(ether ether ketone)/Poly(aryl ether sulfone) Blends

Bhanu Nandan, L. D. Kandpal, G. N. Mathur

Polymer Science Division, Defence Materials & Stores Research & Development Establishment, DMSRDE P.O., GT Road, Kanpur 208013, India

Received 29 July 2002; accepted 12 February 2003

ABSTRACT: The crystallization and melting behavior of poly(ether ether ketone) (PEEK) in blends with poly(aryl ether sulfone) (PES) prepared by melt mixing are investigated by differential scanning calorimetry (DSC) and wide-angle X-ray scattering (WAXS). The presence of PES is found to have a notable influence on the crystallization behavior of PEEK, especially when present in low concentrations in the PEEK/PES blends. The PEEK crystallization kinetics is retarded in the presence of PES from the melt and in the rubbery state. An analysis of the melt crystallization exotherm shows a slower rate of nucleation and a wider crystallite size distribution of PEEK in the presence of PES, except at low concentrations of PES, where, because of higher miscibility and the tendency of PES to form ordered structures under suitable conditions, a significantly opposite result is observed. The cold crystallization temperature of the blends at low PES concentration is higher then that of pure PEEK, whereas at a higher PES concentration little change is observed. In addition, the decrease in heat of cold crystallization and melting, which is more prevalent in PEEK-rich compositions than in pure PEEK, shows the reduction in the degree of crystallinity because of the dilution effect of PES. Isothermal cold crystallization studies show that the cold crystallization from the amorphous glass occurs in two stages, corresponding to the mobilization of the PEEK-rich and PES-rich phases. The slower rate of crystallization of the PEEK-rich phase, even in compositions where a pure PEEK phase is observed, indicates that the presence of the immobile PES-rich phase has a constraining influence on the crystallization of the PEEK-rich phase, possibly because of the distribution of individual PEEK chains across the two phases. The various crystallization parameters obtained from WAXS analysis show that the basic crystal structure of PEEK remains unaffected in the blend. Further, the slight melting point depression of PEEK at low concentrations of PES, apart from several other morphological reasons, may be due to some specific interactions between the component homopolymers. J Appl Polym Sci 90: 2906–2918, 2003

Key words: poly(ether ketones); poly(ether sulfones); blends; crystallization; miscibility

INTRODUCTION

Polymer blends and composites is a rapidly growing field in polymer science and has attracted a lot of attention in both the academic and industrial communities. The fact that new materials can be developed with good properties in relatively less time and with a minimum investment has encouraged the blending of polymers. Blends of two aromatic engineering polymers have been particularly interesting, because excellent properties have been observed even when the blends are immiscible.[1,2] The good interfacial adhesion because of the interaction between the aromatic rings of these polymers may be one of the reasons for the observed behavior.

Poly(ether ether ketone) (PEEK) is a semicrystalline aromatic engineering polymer, and it has excellent thermal and mechanical properties.[3,4] Blends of PEEK with various polymers have been of interest in recent years. Many investigators have studied blends of PEEK with poly(ether imide),[5,6] poly(aryl ether sulfone) (PES),[7–11] liquid crystalline polymers,[12] poly(phenylene sulfide),[13] and poly(ether ketone).[14,15] Of these blends, those of PEEK and PES are particularly interesting from both the application and academic points of view. The addition of PES into PEEK may increase the glass transition and improve the processibility of the latter, whereas a decrease in the chemical resistance and environmental stress rupture resistance behavior of PES is expected. The fact that PEEK is semicrystalline and PES is amorphous makes their blends interesting for the fundamental study of semicrystalline/amorphous blend systems.

The crystallization behavior of a polymer is important because it ultimately governs many of its crucial properties. The subject of crystallization is concerned with a description of the transformation of amorphous crystallizable polymers into semicrystalline materials from both the phenomenological and more basic molecular viewpoints. The properties of semicrystalline polymers significantly depend upon the kind and dis-

Correspondence to: B. Nandan (bhanunandan@hotmail.com).

Contract grant sponsor: Defence Research & Development Organization, India (to B.N.).

Journal of Applied Polymer Science, Vol. 90, 2906–2918 (2003)

tribution of the crystals, as well as the total crystallinity. Thus, the rational control of properties is possible only through an understanding of the kinetics of crystallization and of the underlying molecular processes. In addition, the study of polymer crystallization gives information about molecular motions and arrangements. The results of such investigations shed light upon polymer crystallizability and polymer morphology, which can be used to produce polymer products with desirable properties. A review of the published literature on the crystallization of polymers in blends and alloys clearly indicates that the crystallization behavior and morphology of the component polymers are significantly modified by the presence of the other component, resulting in significant changes in their morphology.[16] The critical factors governing the extent and direction of change in the crystallinity and rate of crystallization include the miscibility, the glass-transition (T_g) and melting temperatures of the constituent polymers, their relative melt viscosities, and the inherent crystallizibility.

Although the miscibility behavior and mechanical properties of PEEK/PES blends have been studied in some detail, there is a dearth of information regarding their crystallization and melting behavior. Eguizabal et al.[7–9] have done a few limited crystallization studies of PEEK/PES blends and have reported that crystallization of PEEK is unaffected in the presence of PES because of their almost complete immiscibility. However, in sharp contrast, Harris and Robeson[10,11] have reported that the crystallization kinetics of PEEK is affected and becomes slower in the presence of PES because of limited miscibility between the two polymers. We have recently investigated the phase behavior and structure–property relationships of PEEK/PES blends in more detail in order to clarify the ambiguities in their reported miscibility behavior and to establish a better understanding of this blend system. In a previous article the miscibility behavior of both solution and melt mixed blends were discussed, and we reported that these blends do show limited miscibility with the presence of PEEK-rich and PES-rich phases.[17] In the present article we are reporting the crystallization and melting behavior of melt mixed PEEK/PES blends. The studies are carried out using differential scanning calorimetry (DSC) and wide-angle X-ray scattering (WAXS) measurements. It is expected that the data generated during the dynamic and isothermal crystallization behavior of PEEK in PEEK/PES blends may lead to a better optimization of the processing parameters for these blends.

EXPERIMENTAL

Materials

PEEK was synthesized in the laboratory by following a reported procedure.[18,19] The purified polymer was then dried in a vacuum oven at 120°C for 48 h. The inherent viscosity of the synthesized PEEK was measured in an Ostwald viscometer at 25°C using 98% sulfuric acid as a solvent (concentration = 1.00 g polymer/100 mL solvent), and the value was found to be 0.81 dL/g. The polymer has the following general structure:

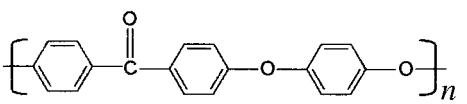

PES was procured from Amoco Performance Products Inc. under the trade name Radel (grade A-300). Although the structure of this polymer has not been disclosed by the manufacturers, Ghosal et al.[20] found it to have the following repeating units in its general structure:

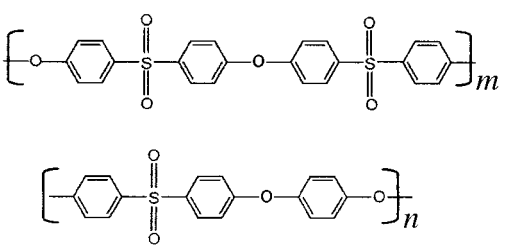

The m/n ratio probably varies in different grades of Radel A PES that are available. Hence, the PES used in the present study is essentially a copolymer of poly(ether ether sulfone) and PES. Some of the important characteristics of the PES and PEEK used in this investigation are listed in Table I.

TABLE I
Characteristics of Polymers

Characteristics	PEEK	PES
$\bar{M}_w$	34,700[a]	42,500[b]
Density (g/cm^3)	1.263[c]	1.370[b]
T_g (°C)	147.6[c]	≈223.0[d]
T_m (°C)	339.1	—

[a] The molecular weight measured in our lab.
[b] The data provided by the manufacturers.
[c] The data for completely amorphous samples.
[d] This varies slightly with the thermal history.

Preparation of blends

PEEK and PES were blended in ratios of 100/0, 90/10, 75/25, 50/50, 25/75, 10/90, and 0/100 (w/w). Before blending, the two polymers were completely dried overnight in an air-circulated oven at 150°C. They were melt blended in a Maxwell mixing extruder (model CS-194 AV, Custom Scientific Instruments), which is a laboratory mixing extruder featuring a screwless design. It has a 0.75-in. diameter rotor and

produces a throughput in the range of 200 g/h. The use of this extruder is discussed elsewhere.[21]

Before melt blending, the two polymers in appropriate weight ratios were thoroughly mixed by hand and then fed into the hopper of the mixing extruder in small batches. The temperatures of both the rotor and die zone were set at 350°C, and a rotor speed of 90 rpm was used for all blend compositions. The total residence time of the polymer mixture inside the mixing zone was approximately 30 s, and extrudates were obtained through a die with a 3.5-mm diameter. The extrudates were further chopped into small granules and again passed through the mixing extruder to ensure thorough mixing. These extrudates were then further converted to granules.

Sample preparation for WAXS

Specimens of 0.3-mm thickness were prepared by compression molding in a hydraulic press. Granules of blends prepared in the extruder and kept between two aluminum foils were placed between the platens of the press, which was already heated to 380°C. A pressure of 100 kg/cm^2 was applied at this temperature for 10 min and then the samples were allowed to cool under pressure at room temperature. It was ensured that the thermal history imparted to each specimen remained constant. A representative amorphous specimen of PEEK was prepared by directly quenching the molded specimen at 380°C to ice-water temperature.

Characterization

DSC measurements

Nonisothermal cold crystallization studies. The effects of blending on the nonisothermal cold crystallization behavior of the component homopolymers were assessed by a DSC 2910 differential scanning calorimeter (TA Instruments) equipped with a model 2100 thermal analyzer (Du Pont Instruments). Calibration for temperature and heat flow (at a scanning rate of 20°C/min) was made prior to sample analysis using indium, tin, and zinc. Each sample (10 ± 2 mg) was first heated at 20°C/min from room temperature to 380°C, which is well above the melting point of the material, and then kept at this temperature for 4 min to ensure complete melting of crystals. Then, the sample was removed from the DSC cell and quickly quenched into liquid nitrogen to obtain an amorphous structure in the samples. In this way any influence of previous thermal history was erased. A second thermal scan was carried out on each sample with the same conditions as in the first scan. The DSC cell was continuously purged with nitrogen during the heating scans.

Nonisothermal melt crystallization studies. Nonisothermal crystallization studies were done using a Perkin–Elmer DSC 7. Samples in the DSC cell were scanned at a rate of 20°C/min up to 380°C. They were kept at this temperature for 4 min, and then the DSC thermogram was recorded in cooling mode at 10°C/min. The crystallization exotherm obtained in this scan was analyzed for various crystallization parameters.

Isothermal crystallization studies. On some of the amorphous samples, obtained as described earlier after the first scan, processes of isothermal crystallization were performed. The DSC cell was first heated to the desired crystallization temperature; as soon as the crystallization temperature was reached, the DSC cell was opened and the sample was kept inside it. After a given equilibration time, which the DSC takes for again reaching crystallization temperature, the DSC thermogram was recorded isothermally. Data were recorded at the crystallization temperature for 30 min, which was long enough to allow the development of complete crystallization at that temperature. Then, the temperature was raised at 20°C/min to 380°C, and the melting enthalpy was calculated. Because there was little variation in the glass-transition temperature with composition, the same isothermal crystallization temperatures (165 and 168°C) were selected for each sample. Each test was performed at least twice and the results averaged.

WAXS studies

A Philips X-pert model X-ray powder diffractometer was used for obtaining X-ray data. Radial scans of intensity I versus 2θ were recorded in the range of $10-60°$ 2θ under identical settings of the instrument using nickel filtered CuK_α radiation with a wavelength of 1.5418 Å. An operating voltage of 40 kV and filament current of 30 mA were used. Data were collected in continuous mode with a step size of $0.02°$ 2θ S^{-1}.

RESULTS AND DISCUSSION

DSC study

A number of parameters signifying the crystallization and melting behavior of the homopolymers and their blends can be determined from the heating and cooling scans in a differential scanning calorimeter. These include the temperature of the onset of melting, the melting peak temperature, the melting temperature range or width of the melting peak, the heat of fusion, the onset of cold crystallization, the crystallization peak temperature, and the heat of cold crystallization from the heating scans, and various melt crystallization parameters from the cooling scans, which are discussed in subsequent sections.

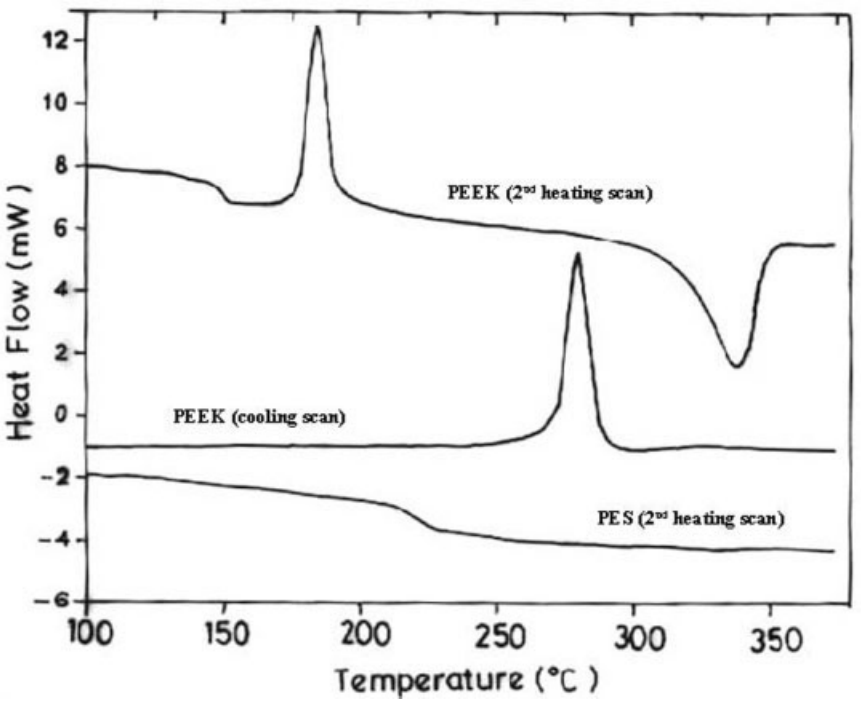

Figure 1 DSC thermograms of PEEK and PES.

Crystallization and melting behavior of homopolymers

Figure 1 shows the DSC reheating and cooling scans for pure PEEK but only the reheating scan for pure PES. The reheating scan of PEEK gives a well-defined exotherm at around 185°C, which corresponds to its cold crystallization. The melting endotherm of PEEK appears at around 340°C. The cooling scan of pure PEEK gives a crystallization exotherm below 300°C. Because PES is an amorphous polymer, it only shows a glass transition in its reheating scan.

Crystallization and melting behavior of blends

Nonisothermal melt crystallization behavior. The nonisothermal melt crystallization behavior was studied from the cooling scans of the homopolymers and their blends. The cooling scans of PEEK/PES blends give a well-developed crystallization exotherm of PEEK below 300°C. The analysis of the model crystallization exotherm presented below adequately describes the crystallization process in a polymer. A comparison of these crystallization exotherms recorded under identical experimental conditions and normalized for identical sample weight leads to information about the crystallization behavior of PEEK in various compositions of the PEEK/PES blend. This analysis is based on the changes in the exotherm parameters defined in Figure 2 on a schematic exotherm. These parameters and their relationships with the crystallization process and morphology are as follows[22]:

1. S_i, the initial slope of the exotherm. This is influenced by the initial process of crystallization, namely, nucleation. The faster the nucleation, the greater will be the S_i value.
2. ΔW, the width of the exotherm at its half-height. This is dependent on the crystallite size distribution such that the narrower the crystallite size distribution, the smaller is the ΔW value.
3. ΔH_c, the exothermic heat of crystallization, which is proportional to the degree of crystallinity.
4. T_{onset}, the temperature at which the thermogram departs from the baseline at the beginning of the exotherm. Its higher value implies the occurrence of the process at a higher temperature, which is an indication of the faster rate process. Supercooling, $(T_m - T_{\text{onset}})$, where T_m is the melting temperature, is known to govern the rate of crystallization and the morphology.
5. T_p, the exotherm peak temperature. This is dependent on the overall rate of crystallization, $(T_{\text{onset}} - T_p)$, which gives how fast the crystallization process is.

This five-parameter model of analysis on the melt crystallization exotherm provides information on the crystallization behavior and the resulting morphology of the crystalline phase of a semicrystalline polymer. However, its essential requirement is that the exotherms be recorded under identical experimental conditions. Self-consistency of this model of analysis is

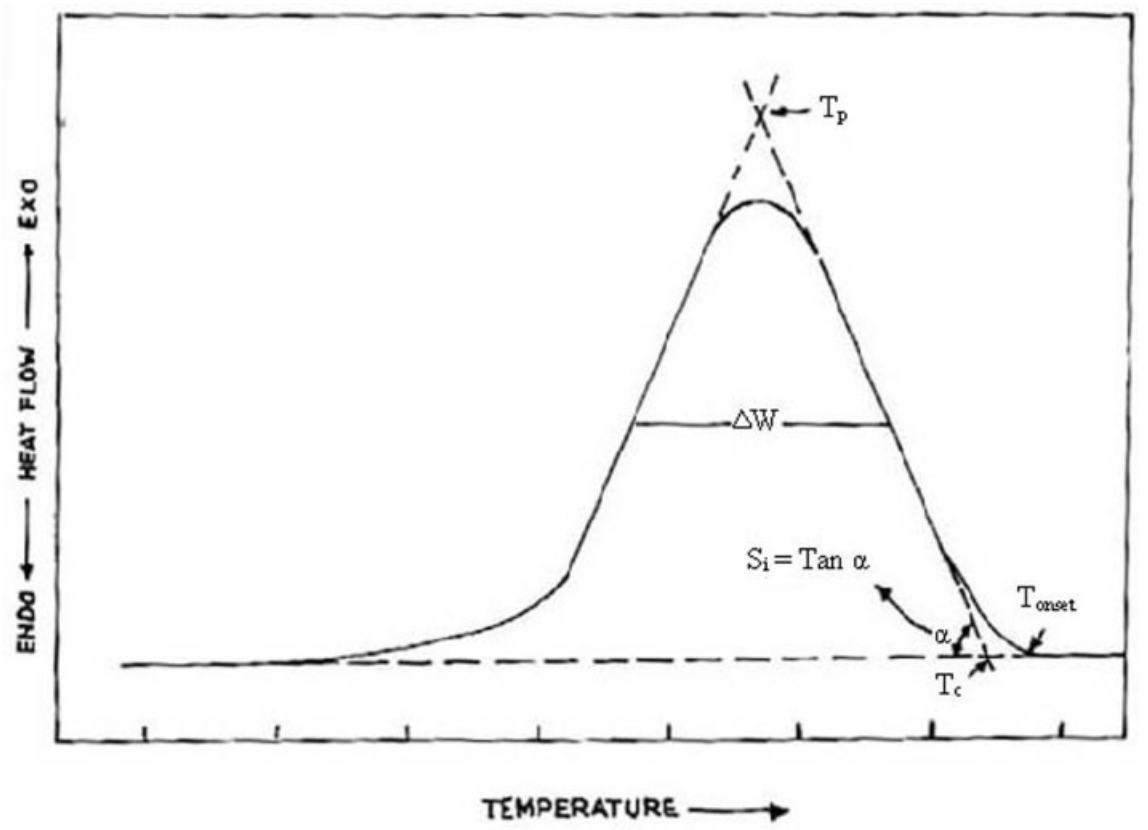

Figure 2 A schematic diagram of a crystallization exotherm recorded during the cooling cycle and the various parameters characterizing it.[22]

inherent in the mutually opposite variation of S_i and ΔW, which implies that an increase of S_i (i.e., an increase of the rate of nucleation) should result in a decrease of ΔW (i.e., a narrower distribution of the crystallite size). The reason for this is that faster nucleation involves an almost simultaneous creation of most crystallites that in subsequent growth produce a narrow crystallite size distribution, whereas slow nucleation involves the creation of nuclei at different times that subsequently grow to widely varying sizes and thus produce a widely distributed crystallite size. This self-consistency has been obeyed in some of the previously studied blend systems.[23–25]

Figure 3 shows the melt crystallization exotherms of pure PEEK and its blend with PES. The various parameters obtained from these exotherms are listed in Table II. The onset temperature of crystallization (T_{onset}) and peak temperature of crystallization (T_p) of PEEK show a continuous decrease with an increase in the PES content in the blend, which demonstrates the retarding influence of PES on the crystallization rate of PEEK. The decrease in the crystallization rate with an increasing concentration of PES is also evident from the degree of supercooling required for initiating crystallization, which shows a continuous increase with the increase in PES concentration. The S_i value slightly increases in the blend composition range from 0 to 25 wt % PES content, and thereafter it decreases. This means that PES at a low concentration increases the nucleation rate, whereas at a high concentration it decreases the nucleation rate appreciably. Thus, at a higher PES concentration the decrease of T_{onset} is accompanied by a slow rate of nucleation, thereby confirming a kinetically slower process. This is as expected for an amorphous/semicrystalline polymer blend system, but the increase in the nucleation rate at 10 and 25 wt % PES is quite unusual. This may be due to the previously reported higher compatibility of the blends at these compositions and the tendency of PES to form an ordered structure such as spherulite-like globules under suitable conditions as discussed elsewhere.[26] Therefore, in these compositions, although the PES phase does retard the onset of crystallization, the PES segments present in the PEEK phase may act as nucleation sites and once crystallization starts, because of the presence of these sites, the nucleation rate is higher. In addition, the nucleation at the domain interfaces may also lead to an increase in the nucleation density. It has been suggested that the interfaces of the phase separated polymer blends, which show some miscibility in the amorphous phase, may serve as nucleation sites for crystallization.[27,28] The ΔW varies inversely to S_i. Thus, at 10 and 25 wt % PES the ΔW decreases, showing a narrower crystallite size distri-

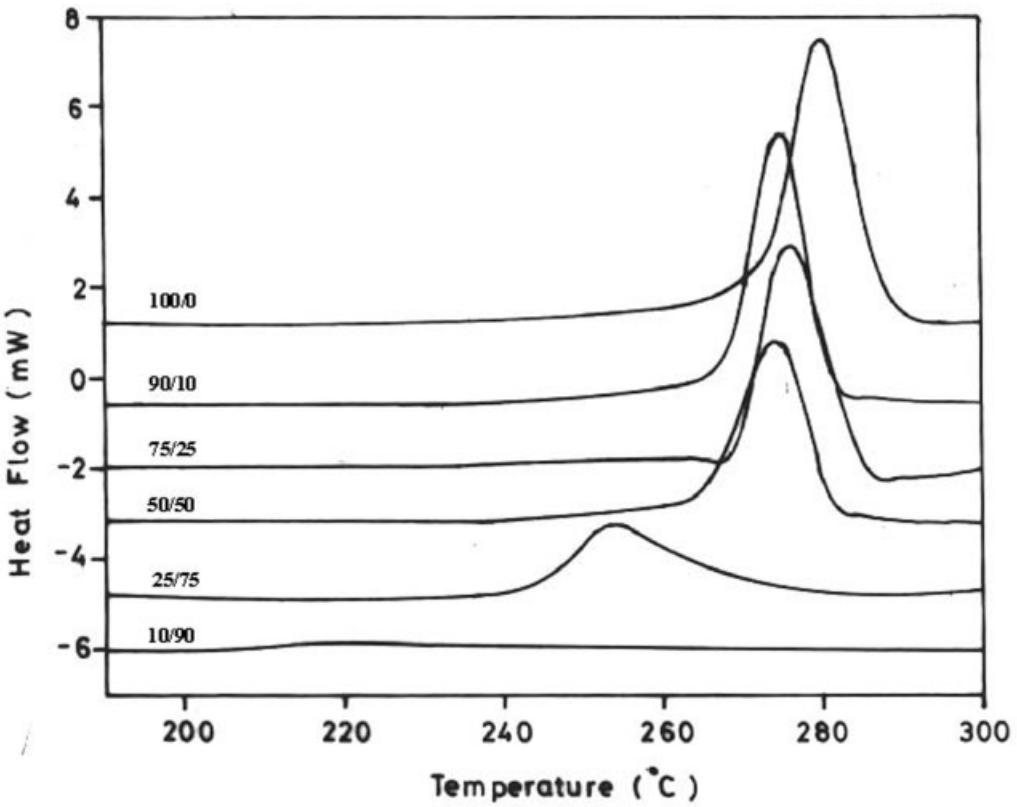

Figure 3 DSC melt crystallization exotherms from the cooling curves of various compositions of PEEK/PES blends.

bution, whereas at higher PES concentrations the ΔW increases, showing a wider crystallite size distribution. This also fulfills the self-consistency condition, which was discussed earlier. The crystallization peak width ($\Delta T = T_{onset} - T_e$) also follows a pattern similar to ΔW. The heat of crystallization (ΔH_c) normalized to the PEEK content in the blend shows a progressive decrease with increasing PES content, indicating that the degree of crystallinity of PEEK is lowered in the blend. This reduction in the degree of crystallinity of PEEK can be explained in terms of the dilution effect of the amorphous PES affecting the crystallization behavior of PEEK. It is the noncrystallizing PES accumulating between the growing fibers of the spherulites and restricting growth that ultimately lowers the rate of crystallization; the noncrystallizing impurities are rejected at the growing front, and at high concentrations of PES the diffusion of PEEK to the growing crystal face will determine the rate.

Nonisothermal cold crystallization behavior. Figure 4 shows the crystallization exotherms of different compositions of PEEK/PES blends obtained after a second heating scan. Second heating scans on liquid nitrogen quenched amorphous samples of PEEK/PES blends show a cold crystallization exotherm of PEEK near 180°C, the position and intensity of which was found

TABLE II
Variation of Various Melt Crystallization Exotherm Parameters Obtained from DSC Cooling Curves of PEEK/PES Blends

Blend Compositions	ΔT_s (°C)	T_{onset} (°C)	T_p (°C)	T_e (°C)	ΔT (°C)	S_i	ΔW (°C)	ΔH_c (J/g)
100/0	45.8	287.7	280.8	273.1	14.6	5.8	8.3	42.6
90/10	48.0	280.4	274.6	268.1	12.3	5.9	7.1	39.7
75/25	50.3	282.5	276.6	270.9	11.6	6.0	6.5	37.7
50/50	50.3	280.9	273.8	264.0	16.9	5.0	8.2	37.6
25/75	50.9	275.0	252.3	240.2	34.8	3.1	18.0	34.0
10/90	52.1	261.1	220.0	204.6	56.5	0.4	31.2	27.0
0/100	—	—	—	—	—	—	—	—

ΔT_s, degree of supercooling; T_{onset}, onset temperature for crystallization; T_p, peak temperature for crystallization; T_e, temperature for completion of crystallization; ΔT, width of crystallization exotherm; S_i, initial slope of the exotherm; ΔW, width of exotherm at half height; ΔH_c, heat of crystallization normalized to the PEEK weight fraction in the blend.

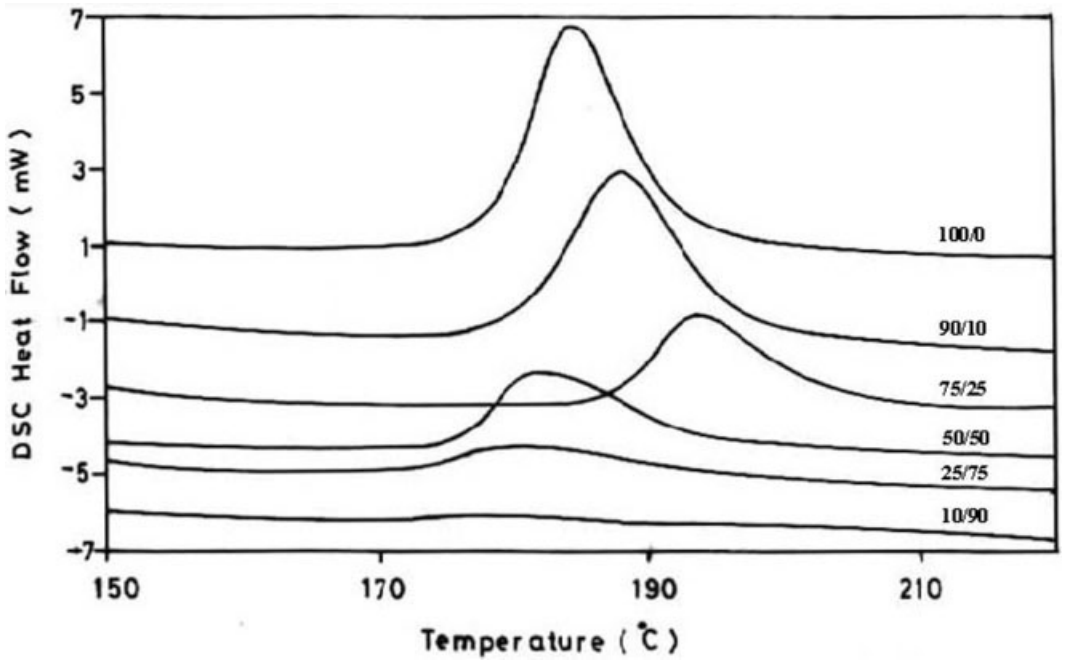

Figure 4 DSC cold crystallization exotherms from the heating curves of PEEK/PES blends.

to vary with the composition. Table III shows various nonisothermal cold crystallization parameters obtained from Figure 4. Both the onset (T_{oc}) and peak (T_{pc}) temperatures for cold crystallization were found to increase as the PES concentration in the blend increases up to 25 wt %. Any further increase in the PES concentration does not result in a significant change in the T_{oc} and T_{pc} values, and they remain almost the same or lower than those of pure PEEK. The increase in T_{oc} and T_{pc} at low concentrations of PES may be because of the increase in the T_g of the PEEK-rich phase in these compositions, which is due to their better miscibility characteristics as discussed elsewhere.[17] Similarly, the decrease in T_{oc} and T_{pc} at high

TABLE III
Nonisothermal Cold Crystallization and Melting Parameters for PEEK in PEEK/PES Blends

Blend Compositions	T_{oc} (°C)	T_{pc} (°C)	ΔH_{cc} (J/g)	T_{om} (°C)	T_{pm} (°C)	T_{cm} (°C)	ΔT (°C)	ΔH_f (J/g)
100/0								
First heating	—	—	—	319.9	341.7	352.1	32.2	37.1
Second heating	178.4	184.6	23.9	316.8	339.1	350.0	33.2	37.2
90/10								
First heating	—	—	—	319.0	339.2	350.0	31.0	33.2
Second heating	180.1	187.7	16.2	315.1	337.4	349.3	34.2	28.0
75/25								
First heating	—	—	—	319.3	338.4	351.1	31.8	31.0
Second heating	185.3	191.9	10.7	315.6	337.7	350.0	34.4	28.5
50/50								
First heating	—	—	—	319.6	339.9	351.2	31.6	30.8
Second heating	175.5	181.6	18.6	317.9	339.2	350.3	32.4	28.5
25/75								
First heating	—	—	—	318.6	338.2	350.2	31.6	26.8
Second heating	171.6	179.3	20.0	312.7	335.6	348.6	35.9	37.0
10/90								
First heating	—	—	—	—	—	—	—	—
Second heating	171.4	179.2	15.0	314.9	336.2	348.1	33.2	26.8
0/100	—	—	—	—	—	—	—	—

T_{oc}, onset temperature for cold crystallization exotherm; T_{pc}, peak temperature for cold crystallization exotherm; ΔH_{cc}, heat of cold crystallization normalized to PEEK weight fraction in the blend; T_{om}, onset temperature for melting endotherm; T_{pm}, peak temperature for melting endotherm; T_{cm}, temperature corresponding to completion of melting endotherm; ΔT, melting peak width; ΔH_f, heat of fusion normalized to PEEK weight fraction in the blend.

concentrations of PES may be because of the decrease in the T_g of the PEEK phase in these compositions.[17] The heat of cold crystallization (ΔH_{cc}) normalized to the PEEK weight fraction in the blend decreases significantly as the PES concentration increases up to 25 wt % in the blend. A further increase in the PES concentration results in a decrease of ΔH_{cc} compared to pure PEEK, but the decrease is less than that observed at lower concentrations of PES. The decrease in ΔH_{cc} on blending PEEK with PES may be because of the mobility restrictions that PES imposes on the PEEK chain, because the former is still below its T_g in these conditions. Because at a low concentration of PES the compatibility of the PEEK/PES blend is better and more PES is dissolved in the PEEK phase, there will be more of an effect on the mobility restrictions of PEEK chains toward crystallizing. This results in the comparatively lower values of ΔH_{cc} at these compositions.

Isothermal cold crystallization behavior. PEEK/PES blends were further studied for their isothermal cold crystallization behavior. Because little variation in the glass-transition temperature of the blends has been observed, common isothermal crystallization temperatures (165 and 168°C) were taken for all the compositions. Figure 5(a) shows the isothermal crystallization exotherms obtained at 168°C. For reasons of brevity, the 165°C results are not shown. As can be observed in Figure 5(a), crystallization was very fast for pure PEEK and it was not possible to record the start of crystallization whereas for 90/10 and 75/25 PEEK/PES blends no sharp crystallization exotherm could be recorded. The crystallization process in these compositions was relatively slow. For the 50/50 PEEK/PES blend a sharp crystallization exotherm followed by a broad crystallization exotherm was observed, indicating the probable formation of crystals in two successive stages (i.e., a different nucleation mechanism is active in the presence of amorphous PES). This is much clearer from Figure 5(b), where the isothermal crystallization thermogram of the 50/50 PEEK/PES blend is shown individually. It can be explained that the first crystallization exotherm corresponds primarily to crystallization in the PEEK-rich phase, while the second crystallization exotherm reflects the ongoing crystallization in both PEEK-rich and PES-rich phases. Because the PEEK dissolved in the PES-rich phase will have much slower crystallization kinetics compared to the crystallization of the PEEK-rich phase, the process continues even after the completion of a given isothermal time inside the DSC cell. Such a two-step crystallization was not observed in blend compositions with high PEEK content. In these compositions probably the second stage crystallization has low intensity and hence gets overlapped by the first stage crystallization, which also takes a longer time for its completion. For the 25/75 PEEK/PES blend, no clear crystallization exotherm could be recorded at 168°C because of low PEEK content. Crystallization at 165°C proceeded at a slower rate and the variation observed along the composition range in PEEK/PES blends was similar to that observed at 168°C. Further, the time to develop the maximum rate of crystallization (t_p), which is presented in Table IV, is highest for the 90/10 PEEK/PES blend, showing that the crystallization process is slowest for this composition as far as the first stage of crystallization in the blends is concerned. This is in agreement with the miscibility behavior shown by these compositions. The strong positive shift in the crystallization peak time for the blends compared to pure PEEK may seem somewhat surprising, given the limited miscibility of PES in the PEEK-rich phase. Especially with the 50/50 PEEK/PES composition, where an almost pure PEEK phase has been observed, the measured crystallization peak time should correspond to those of pure PEEK. This suggests that the presence of an immobile PES-rich phase (at the given isothermal conditions) is in some manner constraining crystallization of the PEEK-rich phase. Because PEEK is miscible in the PES-rich phase in the whole composition range, a possible explanation for the constraint imposed on the PEEK-rich phase by the glassy PES-rich phase is the distribution of individual PEEK chains across the two phases. The segregation of some portion of the individual PEEK chains in the immobile PES-rich environment would presumably lead to a significant decrease both in the crystallization rate and in the overall bulk crystallinity, as observed experimentally. A similar kind of behavior has also been observed in PEEK/polyarylate blends.[29] At higher concentrations of PES, because of low PEEK content in the blend, the crystallization exotherm was not recognizable in the given isothermal time and hence it is difficult to compare the data from these compositions.

Melting behavior. Figure 6 shows the melting endotherms obtained after second heating scans of PEEK/PES blends, and Table III lists the temperature and enthalpy of melting recorded for both first and second heating scans. Because PES does not crystallize, the data refer only to the PEEK phase. The onset temperature of melting (T_{om}) of PEEK in the blends was found to be comparable with that of neat PEEK and did not show significant composition dependence, indicating that the stability of the least stable crystallites of PEEK are not significantly affected by blending with PES.

The melting peak temperature (T_{pm}) of PEEK in its blend with PES was found to slightly decrease with composition, both in the first and the second heating scans. According to Martuscelli,[30] in incompatible semicrystalline/amorphous blends, the crystals of the crystallizable component grow in equilibrium with its own melt phase. The presence of separate domains of the uncrystallizable component, dispersed in the melt

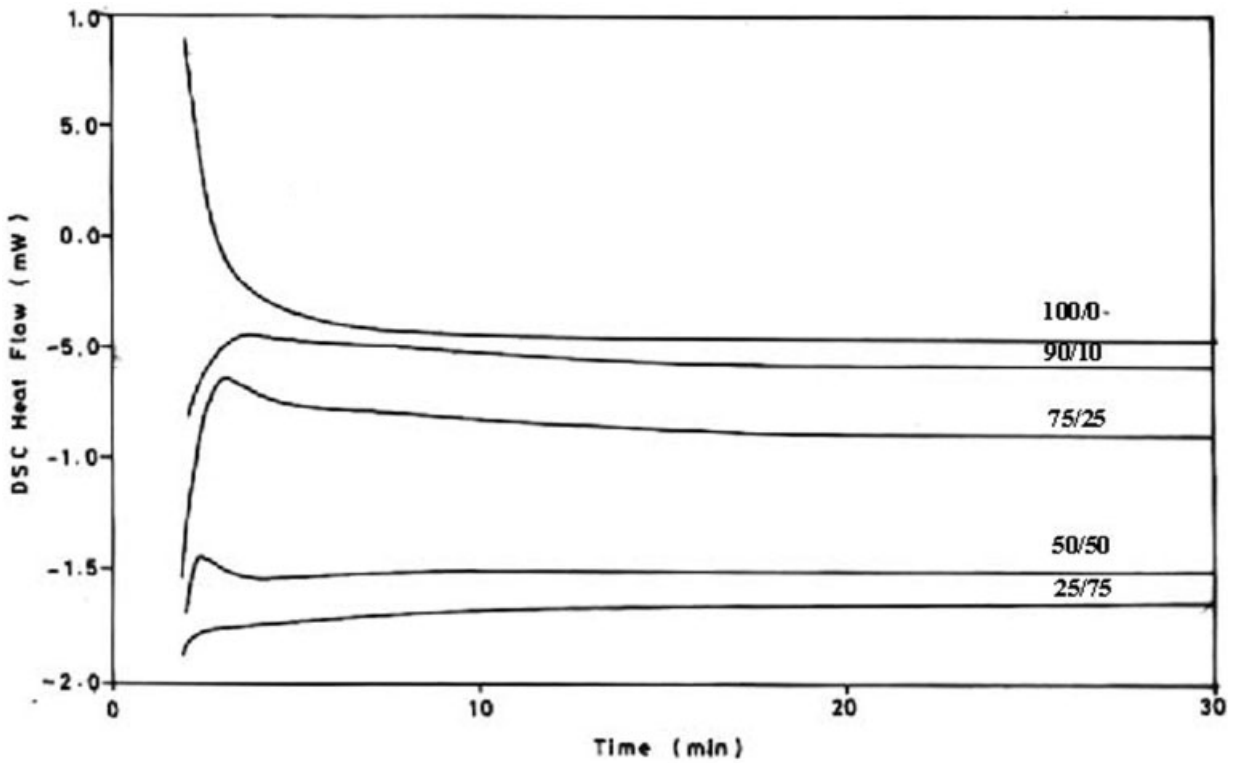

(a)

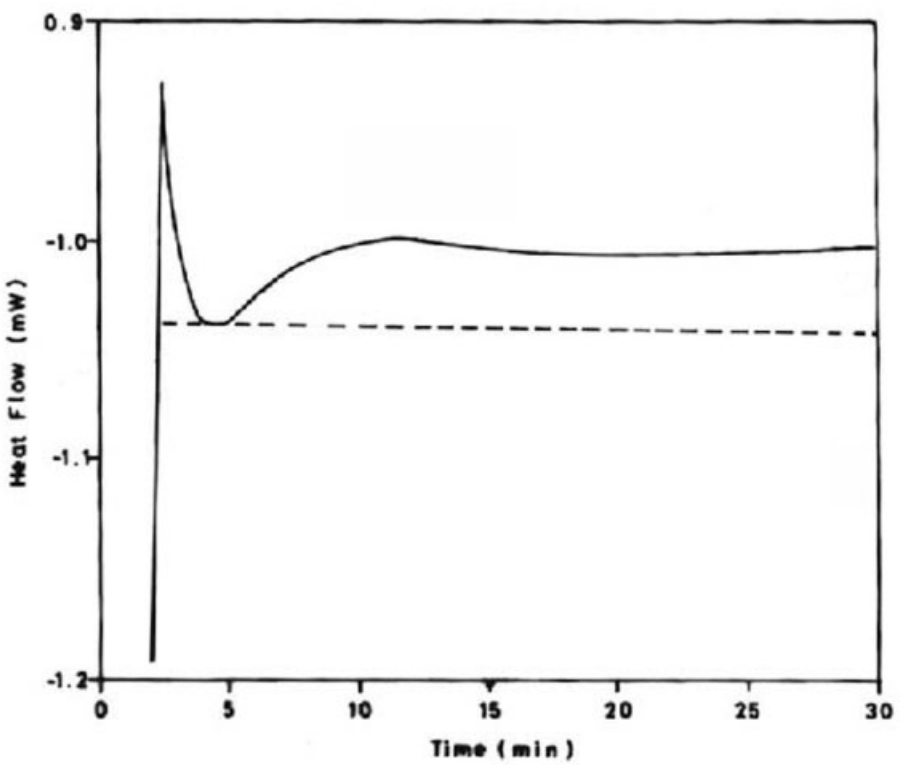

(b)

Figure 5 DSC isothermal crystallization exotherms of (a) various compositions of PEEK/PES blends recorded at 168°C and (b) a PEEK/PES 50/50 blend showing the two-stage crystallization process.

TABLE IV
Isothermal Crystallization Peak Time for Various Compositions of PEEK/PES Blends

Blend Compositions	t_p at 165°C	t_p at 168°C
100/0	Very fast crystallization (induction time not recordable)	Very fast crystallization (induction time not recordable)
90/10	555	104
75/25	274	70
50/50	32 (for first stage)	17 (for first stage)
25/75	Very slow crystallization	Very slow crystallization
10/90	NR	NR
0/100	—	—

t_p, time corresponding to maximum crystallization rate; NR, crystallization not recordable because of a low PEEK concentration in the blend.

matrix during the crystallization process because of kinetic and morphological effects (lamella thickness, defects, spherulitic morphology), may cause a depression of the observed melting temperature, as has been reported by several groups.[31–34] The melting peak width (ΔT_m), which normally is taken as the distribution of crystallite sizes in a semicrystalline polymer, does not show any significant variation. The variation of the heat of fusion (ΔH_f) with composition is in agreement with the observed variation of ΔH_{cc} with composition and it is due to the reason explained in the case of the latter. One interesting observation from Table III is that the heats of fusion of the blends and of pure PEEK are higher than their cold crystallization enthalpy (second heating scan). This means that these samples were not completely amorphous, even if quenched from the melt in liquid nitrogen. In this regard, the pure PEEK is reported to have a very high crystallization rate, and it is possible to obtain it in the amorphous state only when it is quenched at very high cooling rates (1000°C/min).[35] However, one other reason for the difference in the heat of fusion and heat of cold crystallization could be additional, undetected crystallization taking place during the calorimetric scan, as has been reported by others.[36]

WAXS analysis of crystallization behavior

Figure 7 shows the WAXS pattern of as-molded and quenched PEEK and that of as-molded PES. The as-molded PEEK showed several scattering maxima, four of which occurring at 2θ values of 18.78, 20.74, 22.79, and 28.82° were very intense. These peaks correspond to the (1,1,0), (1,1,1), (2,0,0), and (2,1,1) scattering

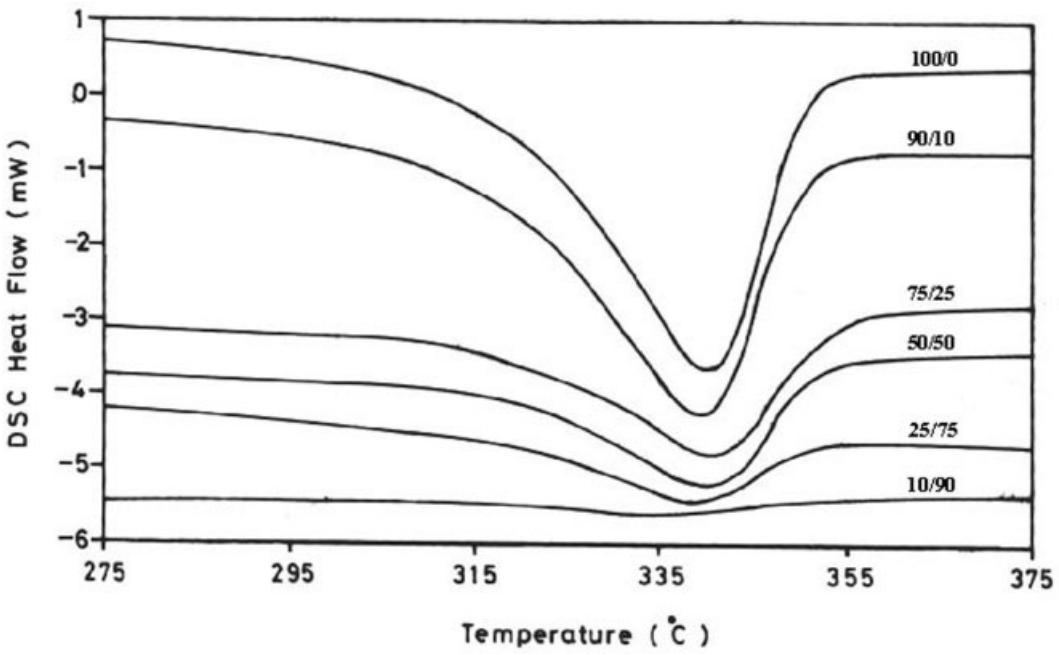

Figure 6 DSC melting endotherms of various compositions of PEEK/PES blends.

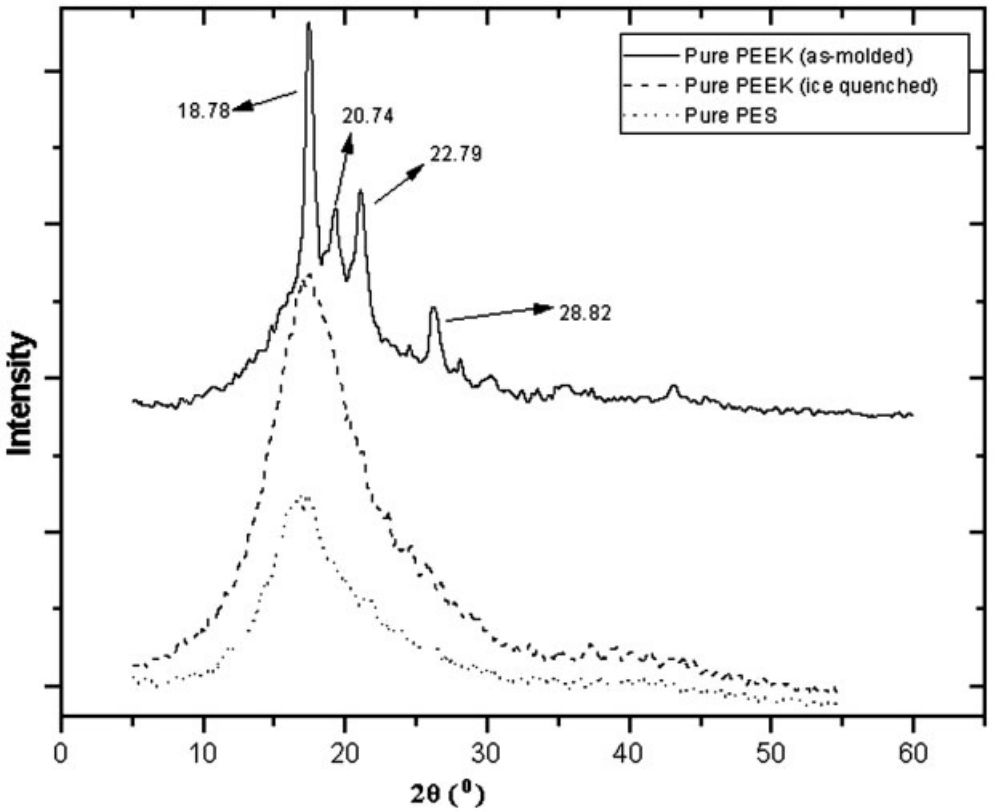

Figure 7 WAXS curves of PEEK and PES.

planes, respectively, of the PEEK crystals with an orthorhombic configuration. These data are in good agreement with those reported by Dawson and Blundell for the PEEK crystal unit cells.[37] The ice-water quenched PEEK shows only a broad amorphous halo in its X-ray scattering pattern, which demonstrates its amorphous nature. The amorphous nature of ice-quenched PEEK samples signifies that the difference between the heat of fusion and the heat of cold crystallization observed in the heating scans of liquid nitrogen quenched PEEK samples is more probably because of undetected crystallization taking place during the calorimetric scan. Further, the X-ray scattering pattern of PES shows an amorphous halo, indicating that no crystallization occurs in this polymer.

The WAXS was performed on as-molded PEEK/PES blends to investigate whether the crystal form of PEEK is influenced or altered when blended with PES. Figure 8 shows the WAXS patterns of as-molded PEEK/PES blends. The figure indicates that no structural change occurs in PEEK crystals with the incorporation of PES in it because the positions of peaks corresponding to different scattering planes of PEEK crystals remain virtually unchanged. Now, the interplanar spacings (d) values for various peaks and the apparent crystal size (L_{hkl}) of PEEK in the direction perpendicular to the (*hkl*) crystal plane can be respectively determined from Bragg's law and Scherrer's equation,[38]

$$D = \lambda/(2\sin\theta) \tag{1}$$

$$L_{hkl} = k\lambda/(\beta_o \times \cos\theta) \tag{2}$$

$$\beta_o = (\beta^2 - b_o^2)^{1/2} \tag{3}$$

where β_o is the half-width of the reflection corrected for the instrumental broadening according to eq. (3), β is the half-width of various scattering peaks, b_o is the instrumental broadening factor (0.15°), λ is the wavelength of radiation, and k is a constant that depends on several factors including the Miller index of the reflecting plane and the shape of the crystal. If the shape is unknown, k is often assigned a value of 0.89.

Table V summarizes the structural parameters determined from WAXS curves using eqs. (1)–(3). It can be seen that the interplanar spacings for various peaks of PEEK show little change with increasing PES concentration. The apparent crystal size of several scattering peaks varies with the PES content, but the variation does not follow any regular trend and it is difficult to conclude anything from the crystal size data.

The WAXS patterns were also used for measuring the mass fraction crystallinity (X_c) in the specimen using the method described by Young.[39] The crystallinity values thus obtained are also listed in Table V. The variation of the X_c from WAXS follows a pattern

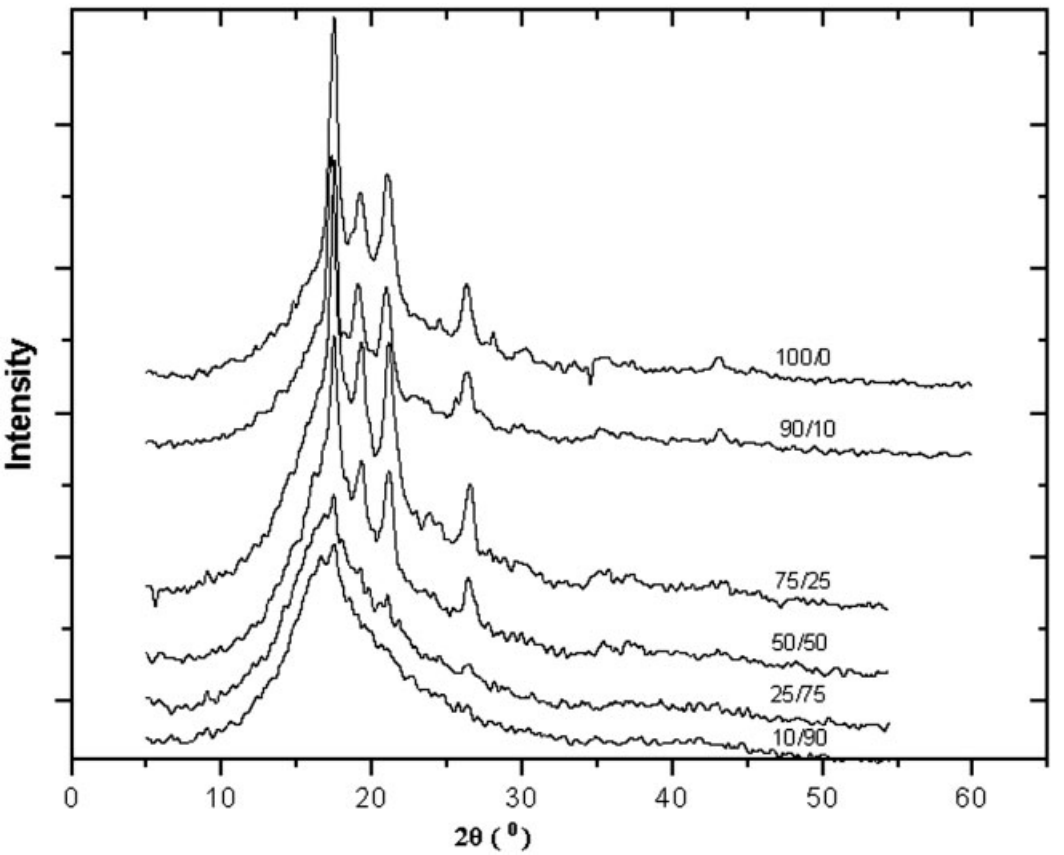

Figure 8 WAXS curves of various compositions of PEEK/PES blends.

TABLE V
Wide Angle X-ray Scattering Data of PEEK in PEEK/PES Blends

Blend Compositions	Crystallinity (%)	Scattering Peaks	2θ	FWHM	Relative Intensity	d Spacing (Å)	L_{hkl} (Å)
100/0	18.5	(1,1,0)	18.78	0.5556	100	4.72	143.33
		(1,1,1)	20.74	0.5928	32.0	4.28	134.74
		(2,0,0)	22.79	0.7769	47.8	3.90	103.17
		(2,1,1)	28.82	0.7065	25.2	3.10	114.82
90/10	16.0	(1,1,0)	18.82	0.5624	100	4.71	141.61
		(1,1,1)	20.80	0.6906	36.7	4.27	115.67
		(2,0,0)	22.88	0.6542	42.0	3.88	122.54
		(2,1,1)	28.86	0.6416	24.2	3.09	126.45
75/25	15.5	(1,1,0)	18.83	0.5928	100	4.71	146.73
		(1,1,1)	20.84	0.6815	36.3	4.26	117.22
		(2,0,0)	22.89	0.8300	53.5	3.88	96.58
		(2,1,1)	28.83	0.7654	27.3	3.09	105.99
50/50	16.5	(1,1,0)	18.81	0.4974	100	4.71	160.11
		(1,1,1)	20.79	0.6434	37.8	4.27	124.15
		(2,0,0)	22.90	0.8018	59.5	3.88	99.98
		(2,1,1)	28.85	0.9024	29.9	3.09	89.90
25/75	11.0	(1,1,0)	18.76	0.5446	100	4.73	146.23
		(1,1,1)	—	—	—	—	—
		(2,0,0)	22.82	1.0795	26.6	3.89	74.25
		(2,1,1)	28.93	1.3692	22.7	3.08	59.26
10/90	—	—	—	—	—	—	—
0/100	—	—	—	—	—	—	—

FWHM, full width at half-maximum; L_{hkl}, the apparent crystal size of PEEK in the direction perpendicular to the (*hkl*) crystal plane.

similar to that measured from DSC. The X_c value decreases in the blend compared to pure PEEK, but the decrease is much more with 10 and 25 wt % PES in the blend for the reasons already discussed.

CONCLUSIONS

The crystallization and melting behavior of PEEK/PES blends prepared by melt mixing were studied using DSC and WAXS. The results show that the crystallization behavior of PEEK is affected in the presence of PES. The presence of amorphous PES had a marked influence on the rate of crystallization of PEEK in the blends: the PES retarded PEEK crystallization both from the melt and in the rubbery state. The effect was found to be more at low concentrations of PES in the blend, because there is more miscibility between the two polymers in these compositions. An analysis of the melt crystallization exotherm shows a slower rate of nucleation and a wider crystallite size distribution of PEEK in the presence of PES, except at low concentrations of PES, where, because of higher miscibility and the tendency of PES to form ordered structures under suitable conditions, this results in a significantly opposite result. The onset and peak temperature for cold crystallization show an increase at low PES concentrations because of the increase in the T_g of the PEEK-rich phase in these compositions. Isothermal cold crystallization studies show a significant decrease in the rate of crystallization with PEEK-rich compositions, where the peak time of crystallization has a higher value. In addition, two distinct crystallization exotherms were observed, more clearly at the 50/50 composition. The second crystallization exotherm reflects ongoing crystallization in both the PEEK-rich and PES-rich phases. The slower rate of crystallization of the PEEK-rich phase compared to pure PEEK also indicates that the presence of the immobile PES-rich phase had a constraining influence on the crystallization of the PEEK-rich phase, possibly because of the distribution of individual PEEK chains across the two phases. The decrease in the heat of cold crystallization and the heat of fusion in blends compared to pure PEEK shows the reduction in the degree of crystallinity of PEEK because of the dilution effect of the amorphous PES. The degree of crystallinity obtained from our WAXS analysis also supports the above results. The various crystallization parameters obtained from the WAXS analysis show that the basic crystal structure of PEEK remains unaffected in the blend. The melting point depression of PEEK at low concentrations of PES signifies the higher miscibility of PEEK/PES blends at these compositions and the possible presence of some interactions between the two polymers.

The authors gratefully acknowledge the help extended by Mr. Amitabh Chakraborty in running the DSC experiments. The first author (B.N.) wishes to express his thanks to the Defence Research & Development Organization, India, for awarding him a Senior Research Fellowship.

References

1. Paul, D. R.; Newman, S. Polymer Blends; Academic: London, 1978; Vols. I and II.
2. Utracki, L. A. Polymer Blends and Alloys: Thermodynamics and Rheology; Hanser: Munich, 1989.
3. Dillon, H. J. Ketone Based Resins: PEEK; Modern Plastics Encyclopedia; McGraw–Hill: New York, 1988; p 48.
4. Velisaris, C. N.; Seferis, J. C. Polym Eng Sci 1986, 26, 1574.
5. Harris, J. E.; Robeson, L. M. J Appl Polym Sci 1988, 35, 1877.
6. Grevecoeur, G.; Greoeninckx, G. Macromolecules 1991, 24, 1190.
7. Arzak, A.; Eguiazabal, J. I.; Nazabal, J. J Mater Sci 1991, 26, 5939.
8. Arzak, A.; Eguiazabal, J. I.; Nazabal, J. J Appl Polym Sci 1995, 58, 653.
9. Eguiazabal, J. I.; Gaztelumendi, M.; Nazabal, J. Recent Res Dev Polym Sci 1998, 2, 113.
10. Harris, J. E.; Robeson, L. M. Eur. Pat. 0,176,989, 1986.
11. Harris, J. E.; Robeson, L. M. Eur. Pat. 0,176,988, 1986.
12. Mehta, A.; Isayev, A. I. Polym Eng Sci 1991, 31, 963.
13. Mai, K.; Mei, Z.; Xu, J.; Zeng, H. J Appl Polym Sci 1997, 63, 1001.
14. Sham, C. K.; Guerra, G.; Karasz, F. E.; McKnight, W. J. Polymer 1988, 29, 1016.
15. Nandan, B.; Lal, B.; Pandey, K. N.; Alam, S.; Kandpal, L. D.; Mathur, G. N. Eur Polym J 2001, 37, 2147.
16. Nadkarni, V. M.; Jog, J. P. In Handbook of Polymer Science and Technology; Cheremisinoff, N. P., Ed.; Marcel Dekker: New York, 1989; Vol. 4, Chapter 3.
17. Nandan, B.; Kandpal, L. D.; Mathur, G. N. J Polym Sci Polym Phys Ed 2002, 40, 1407.
18. Attwood, T. E.; Dawson, P. C.; Freeman, J. L.; Hoy, L. R. J.; Rose, J. B.; Staniland, P. A. Polymer 1981, 22, 1096.
19. Dubey, R.; Singh, R. P.; Tewary, A. K.; Alam, S.; Kandpal, L. D. In Proceedings of the Indian SAMPE Symposium—Bangalore, 1993; Vol. 1, p 27.
20. Ghosal, K.; Chern, R. T.; Freeman, B. D. J Polym Sci Polym Phys Ed 1993, 31, 891.
21. Custom Scientific Instruments. Instruction Manual, Laboratory Mixing Extruder, Model CS-194 AV; Custom Scientific Instruments, NJ, 1994.
22. Jafari, S. H.; Gupta, A. K. J Appl Polym Sci 1999, 71, 1153.
23. Gupta, A. K.; Purwar, S. N. J Appl Polym Sci 1984, 29, 1595.
24. Gupta, A. K.; Gupta, V. B.; Peters, R. H.; Harland, W. G.; Berry, J. P. J Appl Polym Sci 1982, 27, 4669.
25. Gupta, A. K.; Rana, S. K.; Deopura, B. L. J Appl Polym Sci 1992, 44, 719.
26. Xu, J.; Xian, W.; Zeng, H. Polym Commun 1991, 32, 336.
27. Stein, R. S. Mater Res Soc Symp Proc 1994, 321, 531.
28. Chen, H. L. Macromolecules 1995, 28, 2845.
29. Krishnaswamy, R. K.; Douglass, S. K. Polym Eng Sci 1996, 36, 786.
30. Martuscelli, E. Polym Eng Sci 1984, 24, 8.
31. Keith, H. D.; Padden, F. J. J Appl Phys 1964, 35, 1270.
32. Ong, C. J.; Price, F. P. J Polym Sci Polym Symp 1978, 63, 45.
33. Rim, P. B.; Runt, J. P. Macromolecules 1983, 16, 762.
34. Rim, P. B.; Runt, J. P. Macromolecules 1984, 17, 1520.
35. Velisaris, C. N.; Seferis, J. C. Polym Eng Sci 1986, 26, 1574.
36. Ostberg, G. M. K.; Seferis, J. C. J Appl Polym Sci 1987, 33, 29.
37. Dawson, P. C.; Blundell, D. J. Polymer 1980, 21, 577.
38. Alexander, L. E. X-ray Scattering Methods in Polymer Science; Wiley–Interscience: New York, 1969.
39. Young, R. J.; Lovell, P. A. Introduction to Polymers; Chapman & Hall: London, 1991.